encit 2020

ABCM Associação Brasileira de Engenharia e Ciências Mecânicas

18th Brazilian Congress of Thermal Sciences and Engineering
November 16–20, 2020 (Online)

ENC-2020-0732
DEVELOPMENT AND PARAMETRIC ANALYSIS OF A NUMERICAL WIND FLOW MODEL FOR COMPLEX TERRAIN IN OPENFOAM

Gabriel Barbieri Dumont
Adriane Prisco Petry
Department of Mechanical Engineering, Universidade Federal do Rio Grande do Sul
R. Sarmento Leite, 425, 90050-170, Rio Grande do Sul, Brazil
gabriel.dumont@ufrgs.br
adrianep@mecanica.ufrgs.br

William Corrêa Radünz
Department of Mechanical Engineering, Universidade Federal de Santa Catarina
R. Eng. Agronômico Andrei Cristian Ferreira, 88040-900, Santa Catarina, Brazil
w.radunz@posgrad.ufsc.br

Abstract. *This work is based on the CFD modelling of atmospheric boundary layer flows over complex terrains. The employed CFD toolbox is OpenFOAM, which stands out as a robust open source alternative to conventional programs, and the studied cases involve computational domains based on two real life hills – Askervein Hill in Scotland and Bolund Hill in Denmark, the latter being a highly complex terrain. The model is validated through a simulation in a two-dimensional plain terrain with uniform rugosity, where the atmospheric surface layer profile should remain unchanged; this is achieved by modifying the standard wall functions and altering the constants of the standard $k-\varepsilon$ turbulence model. After validation, the model is applied to computational domains which include the hills, and a sensitivity analysis is undertaken by varying mesh refinement, the employed divergence scheme, and the turbulence model's parameters. The results showed that all models underpredicted the turbulent kinetic energy at the lee of both hills, though the effect is much more pronounced in simulations that used the upwind scheme, probably due to numerical diffusion; however, although the higher-order schemes better predict the steep turbulent kinetic energy gradients, they may also overpredict the velocity gradients in the regions close to the ground. As for the turbulence models, it was shown that determining the constants by fitting meteorological data did not necessarily lead to a better result. In general, especially for regions above 2 meters, simulations that employed modified constants for the $k-\varepsilon$ model and higher-order divergence schemes presented wind profiles that were in better agreement with the measured data, with a relative error under 25% for both hills.*

Keywords: *atmospheric boundary layer, complex terrain, parametric analysis, OpenFOAM*

1. INTRODUCTION

As the study of atmospheric boundary layer dynamics is essential to many fields of engineering and environmental science, there is great interest in developing models that are able to accurately predict such flows. Wind farms are particularly affected by the uncertainties in these predictions, and their relatively small scales mean that topographic factors have great influence on the relevant flow parameters, such as average wind speeds and turbulence intensity. Standard microscale wind flow modelling in the wind power industry is still mostly based on linearized versions of the Navier-Stokes equations, as defined by Jackson and Hunt (1975), which tends to overestimate wind speeds when non-linear phenomena such as the wind speed-up effect over steep hills or flow detachment at the lee side are present. This led to the development of CFD models for microscale wind flow, in which the Reynolds-Averaged Navier-Stokes equations (RANS) are solved by turbulence modelling.

The study conducted by (Raithby *et al.*, 1987) was perhaps the first high-impact publication to use CFD modelling for this purpose, and employed the $k-\varepsilon$ turbulence model, which has since become a staple in CFD modeling of microscale flows. This is in great part due to the work of Richards and Hoxey (1993), which proposed vertical wind speed and turbulence profiles that produce homogeneous wind flow for the $k-\varepsilon$ model. However, despite being consistent with the $k-\varepsilon$ model, there is a known issue where these profiles may change when they ought to remain homogeneous, due to the use of improper wall-functions. This issue was solved by (Balogh *et al.*, 2012) through the development of atmospheric wall-functions consistent with the Richards and Hoxey (1993) homogeneous profiles.

This paper proposes a consistent CFD model for wind flows over complex terrains, based on the open source C++ toolbox OpenFOAM, which stands out as a robust open source alternative to conventional CFD software. The studied

cases involve computational domains based on two real life hills – Askervein Hill in Scotland and Bolund Hill in Denmark, the latter being a highly complex terrain. These hills were chosen as the meteorological data for both of them is widely available and extensively documented in the literature (Taylor and Teunissen, 1987; Bechmann *et al.*, 2011), allowing the validation of the model without need of further measurements.

This work contains modifications of two standard wall-functions in the code, as well as three different methodologies for choosing the turbulence model constants. In order to determine the most practical setting for the model, its sensitivity to these constants is evaluated, in addition to its sensitivity to the grid and to different discretization schemes. In total, 36 simulations are run for Askervein, plus 27 for Bolund, and the results are compared to analyze the model's performance in terrains of varying complexity

2. MATHEMATICAL MODELING

The simulated region is the atmospheric surface layer, which represents the lower 200 m of the atmospheric boundary layer. It is in this region that the wind speed gradients are most intense, due to the proximity to the surface, and the effects of friction and convection have a large influence on the vertical wind speed and temperature profiles in general (Stull, 1988).

Another distinctive quality of this region of the atmosphere is that the turbulent momentum and heat fluxes are somewhat constant along its height, and it is sometimes referred to as the constant flux layer. By neglecting the Coriolis force and the effects of non-neutral thermal stratification, it can adequately be modeled by the steady-state, incompressible RANS equations with the standard $k-\varepsilon$ model, which are present in the OpenFOAM solver *simpleFoam* and shown below in Einstein notation

$$\frac{\partial \overline{u_i}}{\partial x_i} = 0 \tag{1}$$

$$\rho \overline{u_j} \frac{\partial \overline{u_i}}{\partial x_j} = -\frac{\partial \overline{p}}{\partial x_i} + \frac{\partial}{\partial x_j}\left[\mu\left(\frac{\partial \overline{u_i}}{\partial x_j} + \frac{\partial \overline{u_j}}{\partial x_i}\right) - \rho\overline{u_i' u_j'}\right] \tag{2}$$

$$\rho \overline{u_j} \frac{\partial k}{\partial x_j} = \frac{\partial}{\partial x_j}\left[\left(\mu + \frac{\mu_t}{\sigma_k}\right)\frac{\partial k}{\partial x_j}\right] + P_k - \rho\varepsilon \tag{3}$$

$$\rho \overline{u_j} \frac{\partial \varepsilon}{\partial x_j} = \frac{\partial}{\partial x_j}\left[\left(\mu + \frac{\mu_t}{\sigma_\varepsilon}\right)\frac{\partial \varepsilon}{\partial x_j}\right] + \frac{C_{\varepsilon 1}\varepsilon}{k}P_k - \frac{C_{\varepsilon 2}\rho\varepsilon^2}{k} \tag{4}$$

where ρ is the air density [kg/m³], μ is its dynamic viscosity [Pa·s], $\overline{u}$ is the Reynolds-Averaged wind speed [m/s] and $\overline{p}$ is the modified pressure [Pa]. The turbulent kinetic energy (TKE) is given by k [m²/s²], while ε is its dissipation rate [m²/s³] and P_k its production term [W/m³]. The dimensionless model constants are σ_k, σ_ε, $C_{\varepsilon 1}$ and $C_{\varepsilon 2}$; the first two are turbulent Prandtl numbers, while the latter two are related to TKE dissipation.

The turbulent eddy viscosity μ_t [Pa·s] and the Reynolds stress tensor $\overline{u_i' u_j'}$ [m²/s²] are related through the Boussinesq hypothesis

$$\overline{u_i' u_j'} = -\frac{\mu_t}{\rho}\left(\frac{\partial \overline{u_i}}{\partial x_j} + \frac{\partial \overline{u_j}}{\partial x_i}\right) \tag{5}$$

in which the normal Reynolds stresses are incorporated into the Reynolds-Averaged pressure, resulting in the modified pressure $\overline{p}$. The production of TKE is a function of the mean velocity gradient

$$P_k = -\rho\overline{u_i' u_j'}\frac{\partial \overline{u_i}}{\partial x_j} \tag{6}$$

Finally, the turbulent eddy viscosity in the $k-\varepsilon$ model is given by the following expression:

$$\mu_t = \rho C_\mu \frac{k^2}{\varepsilon} \tag{7}$$

where C_μ is the model's final dimensionless constant. Its standard value, along with the standard values of the other dimensionless model constants, is given by Launder and Spalding (1974), and shown below

$$C_\mu = 0.09, \qquad C_{\varepsilon 1} = 1.44, \qquad C_{\varepsilon 2} = 1.92, \qquad \sigma_k = 1.0, \qquad \sigma_\varepsilon = 1.3 \tag{8}$$

The above model may be simplified by employing assumptions, such as constant pressure and shear stress and negligible vertical velocity, which are reasonable considering atmospheric surface flows in flat terrain. Doing so, Richards

and Hoxey (1993) obtained a set of vertical profiles which are a solution to the standard $k-\varepsilon$ model equations, as long as σ_ε satisfies Eq. (12):

$$\overline{u} = \frac{u_*}{\kappa} \ln\left(\frac{z+z_0}{z_0}\right) \tag{9}$$

$$k = \frac{u_*^2}{\sqrt{C_\mu}} \tag{10}$$

$$\varepsilon = \frac{u_*^3}{\kappa(z+z_0)} \tag{11}$$

$$\sigma_\varepsilon = \frac{\kappa^2}{(C_{\varepsilon 2} - C_{\varepsilon 1})\sqrt{C_\mu}} \tag{12}$$

in which z is the height [m], κ is the dimensionless von Kármán constant, u_* is the friction velocity [m/s] and z_0 is the roughness lenght [m].

2.1 Model Verification

Verification of the model's consistency is performed through the simulation of a plain, two-dimensional empty fetch with 10 km along the flow direction, 1.5 km across and uniform rugosity at the bottom. The profiles given by Eqs. (9-11) are applied at the west inlet boundary, while constant pressure is assigned at the east boundary. The appropriate wall-functions (WFs) are applied at the bottom, and inflow values are specified at the top.

Since the aforementioned inflow profiles are a solution to the governing equations, they should remain unaltered through the whole domain; however, they may change if there is an inconsistency between the turbulence model, the inflow profiles and the employed WFs. In wind engineering, it has been shown that the use of classic WFs based on Nikuradse's sand-grain roughness for the ε and μ_t fields does indeed cause flow inhomogeneity, and so (Balogh *et al.*, 2012) proposed the following alterations to the ε WFs:

$$\varepsilon_P = \frac{C_\mu^{0.75} k^{1.5}}{\kappa z_p} \rightarrow \frac{C_\mu^{0.75} k^{1.5}}{\kappa\,(z_p + z_0)} \tag{13}$$

$$P_{k_P} = \frac{\tau_w^2}{\kappa C_\mu^{0.25} k_P^{0.5} z_p} \rightarrow \frac{\tau_w^2}{\kappa C_\mu^{0.25} k_P^{0.5}\,(z_p + z_0)} \tag{14}$$

where the subindex P represents the near-ground cell-center and τ_w is the wall shear stress [Pa].

While OpenFOAM offers a formulation for the μ_t WF that is consistent with the atmospheric inflow profiles, *nutkAtmRoughWallFunction*, the file corresponding to the ε WF, *epsilonWallFunction*, must be rewritten to match the formulation shown in Eqs. (13-14) by adding z_0 to the code. After this change was made, the wind speed profile remained unchanged through the entire domain, confirming the model's consistency. This is shown in Figure 1:

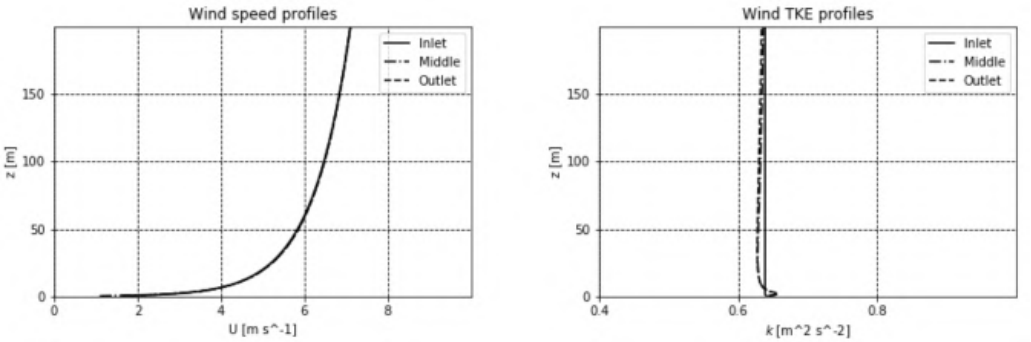

Figure 1. Vertical profiles for wind speed (left) and TKE (right) in the verification domain.

It can be seen that the $\overline{u}$ profile remains constant along all the whole domain. The k profile doesn't change from the middle to the end of the domain, but develops a small peak near the ground from the beginning to the middle. According to Richards and Norris (2011), this does not compromise the homogeneity and is due to an issue with the discretization of the P_k term.

3. DOMAINS AND BOUNDARY CONDITIONS

Two computational domains are employed in this study, one for each hill. Both computational domains consist of a three-dimensional box centered on the hill, with the hills themselves placed far away from the computational boundaries so that errors caused by interactions with the boundary conditions are reduced. For Bolund Hill, meshing is done using the *snappyHexMesh* OpenFOAM application for unstructured grids, and three meshes of increasing refinement are analyzed. For Askervein Hill, meshing is done using the third-party *terrainBlockMesher* package (Schmidt *et al.*, 2012) and four meshes of increasing refinement are analyzed. Table 1 shows the grids employed in the sensitivity analysis, where Z_w is the height of the center of the first cell above the ground.

Table 1. Computational grids employed in the simulations.

Mesh	Number of Volumes	Z_w [m]	Domain Size [km]
Askervein - M1	1,152,000	5.0	6 x 5 x 1.5
Askervein - M2	2,064,860	2.5	6 x 5 x 1.5
Askervein - M3	3,744,000	1.0	6 x 5 x 1.5
Askervein - M4	5,713,200	0.5	6 x 5 x 1.5
Bolund - M1	1,007,129	0.2	0.8 x 0.8 x 0.2
Bolund - M2	1,495,245	0.1	0.8 x 0.8 x 0.2
Bolund - M3	2,301,215	0.05	0.8 x 0.8 x 0.2

The employed boundary conditions also follow the same pattern in both computational domains. The inflow profiles are applied at the western face of the box, while the constant pressure outflow condition is used in the opposite eastern face. The side faces, as well as the top face, employ a *slip* or zero gradient condition, and the consistent WFs are assigned at the ground, along with a *no slip* or zero velocity condition for the $\overline{u}$ field.

It is also worth mentioning that, since the inflow profiles were deduced for a flat terrain, their use in the analysis of atmospheric flow over complex terrain may be called into question. This issue is avoided due to the coastal location of both hills, which means that the incoming wind from the sea should neatly fit the profiles. This is observed, and shown in section 5.

3.1 Askervein Hill

Askervein hill is located in Scotland, in the isle of South Uist, and its geographical coordinates are 57°11'N and 7°22'W. From above, the hill is nearly elliptical, with a minor axis of approximately 1 km and a major axis of 2 km oriented along a NW-SE line. It is a relatively gentle slope with a maximum height of 116 m above the surrounding terrain, and its surroundings consist of plain terrain covered by mostly grass, distant 3 - 4 km from the sea. Considering these factors, Taylor and Teunissen (1987) recommend the use of a uniform roughness of $z_0 = 0.03$ m.

A field measurement campaign was undertaken in 1983, and it employed over 50 masts along lines that crossed the hilltop. This work employed data from a day when the moderate to strong neutrally stratified winds from the sea had a dominant direction of 210º, which differed from the "A" line of masts by only 13º counter-clockwise. Figure 2 shows Askervein Hill and its computational domain, with the horizontal coordinate oriented along the main flow direction, including the "A" line of masts in white.

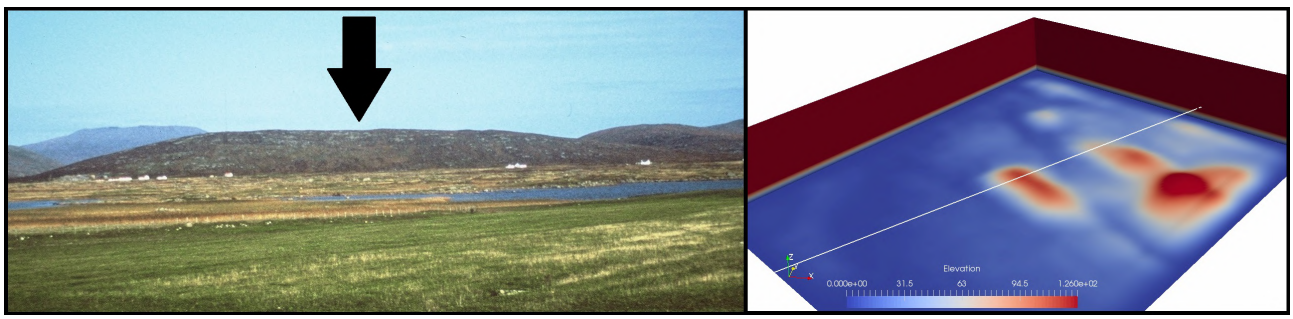

Figure 2. Picture of Askervein (left - Taken from Taylor and Teunissen, 1987) and its computational domain (right).

3.2 Bolund Hill

Unlike Askervein, a relatively smooth hill, Bolund Hill consists of a 12 m escarpment surrounded by sea, which means that the fully-developed, undisturbed wind profiles that come from the sea are met with an abrupt rise in elevation

and surface roughness (Berg *et al.*, 2011). It is, therefore, used to test the model's performance on highly complex terrain; additionally, the Bolund campaign employed masts that measured wind speed and turbulence intensity closer to the ground, at 2 meters and 5 meters. It is situated next to Risø-DTU campus in Roskilde, and its geographical coordinates are 55°42'N and 12°16'E.

The measurement campaign was undertaken between December 2008 and February 2009, and employed 10 masts. In this work, the wind incoming from the west (270°) is simulated and compared to the results from the four masts situated along line "B", which is also oriented along the W-E axis. According to (Bechmann *et al.*, 2011), the sea roughness can be set as $z_0 = 0.0003$ m, while Bolund itself is uniformly covered with grass and has no obstacles, and as such its roughness can be considered uniform and equal to $z_0 = 0.015$ m. Figure 3 presents Bolund and its computational domain, along with the "B" line of masts in white.

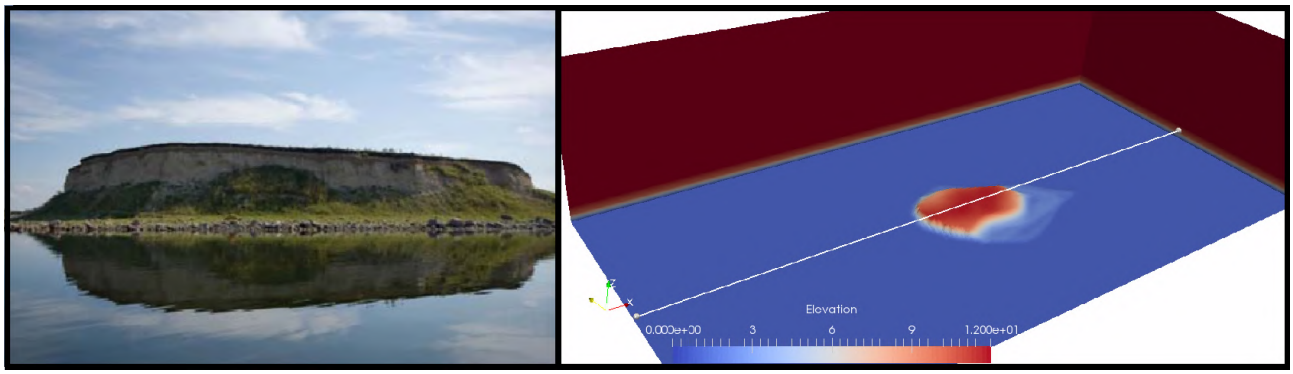

Figure 3. Picture of Bolund (left - Taken from Bechmann *et al.*, 2011) and its computational domain (right).

4. SIMULATION SETTINGS

The *simpleFoam* solver, which is based on the SIMPLE pressure-velocity coupling algorithm, was used with two additional non-orthogonality correctors. For the pressure field, the Generalised Geometric-Algebraic Multi-Grid (GAMG) solver was chosen, as it led to much shorter iteration times than the PCG algorithm without no loss of stability, while the remaining fields employed the Preconditioned Bi-Conjugate Gradient (PBiCG) algorithm. The relaxation factors varied according the the domain and the order of the discretization scheme employed, and are shown in Table 2:

Table 2. Relaxation factors employed in the simulations.

	p	**U**	**k**	ε
Askervein - 1st Order	0.3	0.7	0.7	0.7
Askervein - 2nd Order	0.3	0.7	0.4	0.4
Bolund - 1st Order	0.3	0.7	0.7	0.7
Bolund - 2nd Order	0.3	0.4	0.3	0.3

Finally, the convergence criteria was defined as 10^{-4} for all fields, and all simulations were performed in parallel on a 8 core @ 4 GHz 16-GB-RAM workstation, and took 0.5 to 7 hours to reach convergence.

4.1 Parametric Analysis

Besides the different grids defined in Tab. 1, the model's sensitivity to other input parameters is also analyzed. The standard (or "Std") $k - \varepsilon$ model's constants, defined in Eq. (8), are a good candidate for further analysis, as they were adjusted for engineering-scale flows, and, as such, may be redefined for atmospheric flows. A new set of values is proposed by (Beljaars *et al.*, 1987), which estimates $C_\mu = 0.033$ for atmospheric flows and thus an adjusted value for σ_ε as well; this set of constants is referred to as "Atmospheric" or "Atm" in this work. Another methodology for obtaining the model constants is by isolating C_μ in Eq. (10) and substituting k for a reference value obtained through meteorological measurements on site; this leads to a different adjusted value for σ_ε and the correspondent set of constants is referred to as "Fitted" or "Fit" in this work.

Different discretization schemes are also tested, and of particular interest is the model's response to the use of different interpolation schemes for the non-linear advection term, as lower order schemes tend to introduce more numerical diffusion. As numerical diffusion smoothens gradients, its effects can be very relevant in the near-wall regions, where the wind speed and turbulence kinetic energy gradients are most intense. The analyzed schemes are the first-order upwind and the second-order linearUpwind and QUICK schemes.

In total, three different sets of constants are evaluated ("Std", "Atm" and "Fit"), along with three different divergence schemes ("upwind", "linearUpwind" and "QUICK"), as well as three different grid resolutions for Bolund and four different grid resolutions for Askervein. This results in 27 different cases for Bolund and 36 different cases for Askervein, or 63 cases in conjunction.

As the phenomenon of interest is the variation of wind flow characteristics caused by the presence of complex terrain, the adopted validation parameters are the wind speed ratio (SR) and the turbulent kinetic energy ratio (TKER):

$$SR = \frac{\overline{u}}{\overline{u}_{ref}} \tag{15}$$

$$TKER = \frac{k}{k_{ref}} \tag{16}$$

where the results at a given point in the computational domain, $\overline{u}$ and k, are divided by the value specified by the Eq. (9-10) inlet profiles at the same height - $\overline{u}_{ref}$ and k_{ref}.

The comparison between the measured and simulated values is performed considering two metrics – the relative error between them (e) [%]:

$$e = \frac{\mid \phi_{simu} - \phi_{exp} \mid}{\mid \phi_{exp} \mid} \cdot 100 \tag{17}$$

where ϕ can stand for any field and the subindexes "$simu$" and "exp" denote values obtained through CFD simulation and through the measurement campaign, respectively.

Also employed as a validation parameter is the "hit rate" (HR) [%], which expresses the percentage of simulated values that differ from the measured values by less than 25% or one standard deviation. In other words, if the simulated values are correct in 7 out of 10 positions, the HR for the whole simulation is 70%.

5. RESULTS AND DISCUSSION

As the great number of analyzed cases makes data visualization challenging, the figures and tables below present groups of cases where one of the input parameters is kept fixed and the other two are allowed to change. Considering that the change from a 1st order scheme to a 2nd order one impacted the results considerably more than the choice between linearUpwind and QUICK, Tables 3-4 present the influence of grid refinement considering only the upwind and QUICK schemes, since the linearUpwind results were slightly closer to the upwind ones, as expected. They show the hit rates and average and maximum values for the relative error of both SR and $TKER$.

Table 3. Influence of grid refinement in the Askervein results.

Case - Askervein	HR_{SR} **[%]**	e_{SR} **[%]**	$e_{SR,Max}$ **[%]**	HR_{TKER} **[%]**	e_{TKER} **[%]**	$e_{TKER,Max}$ **[%]**
upwind (M1)	87	21	81	67	23	66
upwind (M2)	87	20	80	70	21	57
upwind (M3)	87	21	80	70	20	52
upwind (M4)	87	21	83	67	21	51
QUICK (M1)	93	16	58	73	20	42
QUICK (M2)	90	18	72	67	19	45
QUICK (M3)	90	18	70	70	19	45
QUICK (M4)	90	19	75	70	19	46

Table 4. Influence of grid refinement in the Bolund results.

Case - Bolund	HR_{SR} **[%]**	e_{SR} **[%]**	$e_{SR,Max}$ **[%]**	HR_{TKER} **[%]**	e_{TKER} **[%]**	$e_{TKER,Max}$ **[%]**
upwind (M1)	54	14	61	33	33	89
upwind (M2)	62	13	49	37	32	88
upwind (M3)	71	15	62	42	31	80
QUICK (M1)	75	12	54	37	30	92
QUICK (M2)	75	18	60	37	29	108
QUICK (M3)	75	17	63	46	25	67

Figure 4 shows a cross-section of the Askervein computational domain, parallel to the direction of the incoming wind. The black dots represent the values measured 10 m above ground by the mast at that position, while the lines represent

the simulated values 10 m above ground for all of the computational domain along the wind direction. The left side shows the results for SR, while the right side shows the results for TKER; to avoid clutter, only the cases ran on the most refined grid (M4) are shown, for every combination of turbulence model constants ("Standard", "Atmospheric" and "Fitted") and discretization schemes ("upwind", "linearUpwind" and "QUICK").

Figure 5 shows the measured data and simulation results in a cross-section of the Bolund domain, in a manner analogous to Fig. 4, and Tables 5-6 complement the above figures by presenting the numerical values associated with them. While Table 5 only uses Askervein data obtained at 10 m from the ground, Table 6 incorporates the measurements at 5 m and 2 m for Bolund.

For Bolund Hill, the vertical SR and TKER profiles are evaluated at every mast, as shown in Fig. 6 and Fig. 7, and compared to the measured values at 2 m and 5 m. For Askervein, the vertical profiles are only evaluated at the hilltop, where measurements at many different heights are available, according to Fig. 8.

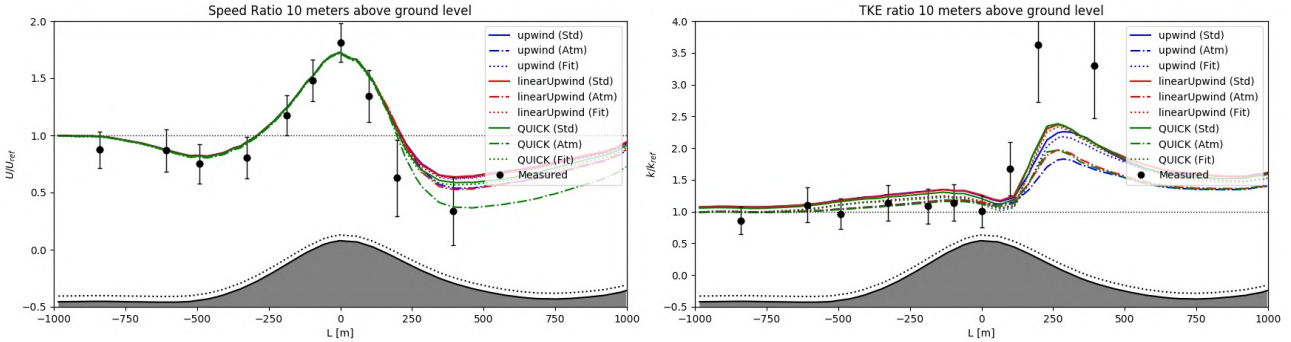

Figure 4. SR and TKER 10 m above ground through the Askervein computational domain.

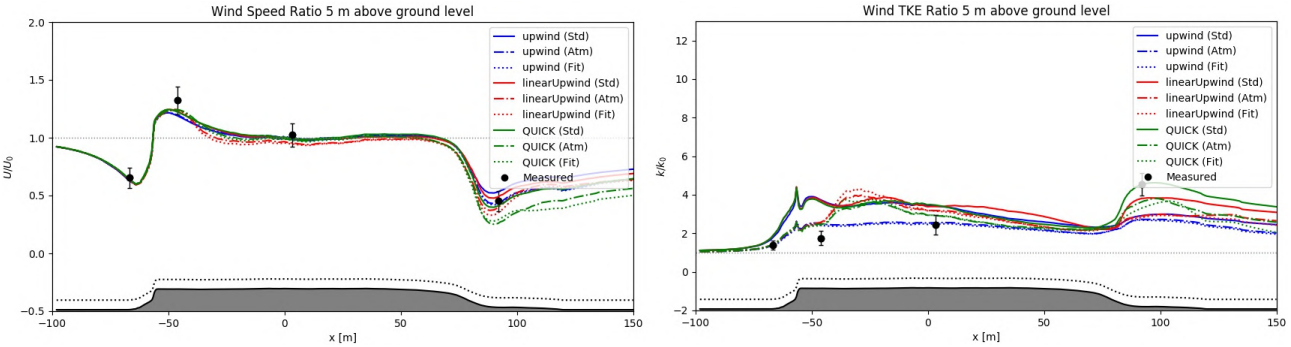

Figure 5. SR and TKER 5 m above ground through the Bolund computational domain.

Table 5. HR and relative error values for Askervein, considering grid M4.

Case - Askervein	HR_{SR} **[%]**	e_{SR} **[%]**	$e_{SR,Max}$ **[%]**	HR_{TKER} **[%]**	e_{TKER} **[%]**	$e_{TKER,Max}$ **[%]**
upwind (Std)	90	22	89	60	23	48
upwind (Atm)	90	19	71	70	19	57
upwind (Fit)	90	22	86	70	20	51
linearUpwind (Std)	80	22	90	50	22	43
linearUpwind (Atm)	90	19	70	70	19	53
linearUpwind (Fit)	90	21	84	70	19	46
QUICK (Std)	90	20	75	70	21	43
QUICK (Atm)	90	13	58	70	18	52
QUICK (Fit)	90	19	69	70	18	44

The results illustrate that the model is quite sensitive to terrain complexity, as the Bolund hill simulations are shown to be more sensitive to all parameters. It can also be seen that the model tends to underpredict the turbulent kinetic energy at the lee of both hills, though the effect is much more pronounced in simulations that used the upwind scheme, probably due to numerical diffusion; however, although the higher-order schemes better predict the steep turbulent kinetic energy gradients, they may also overpredict the velocity gradients in the regions close to the ground. As for the turbulence models, it was shown that determining the constants by fitting meteorological data did not necessarily lead to a better result, and

Table 6. HR and relative error values for Bolund, considering grid M3.

Case - Bolund	HR_{SR} [%]	e_{SR} [%]	$e_{SR,Max}$ [%]	HR_{TKER} [%]	e_{TKER} [%]	$e_{TKER,Max}$ [%]
upwind (Std)	62	18	81	25	40	113
upwind (Atm)	75	12	48	50	26	63
upwind (Fit)	75	14	58	50	26	64
linearUpwind (Std)	87	9	25	25	34	111
linearUpwind (Atm)	75	20	80	62	20	47
linearUpwind (Fit)	62	21	85	50	21	43
QUICK (Std)	75	23	58	50	31	76
QUICK (Atm)	62	28	74	62	22	39
QUICK (Fit)	62	28	76	62	22	46

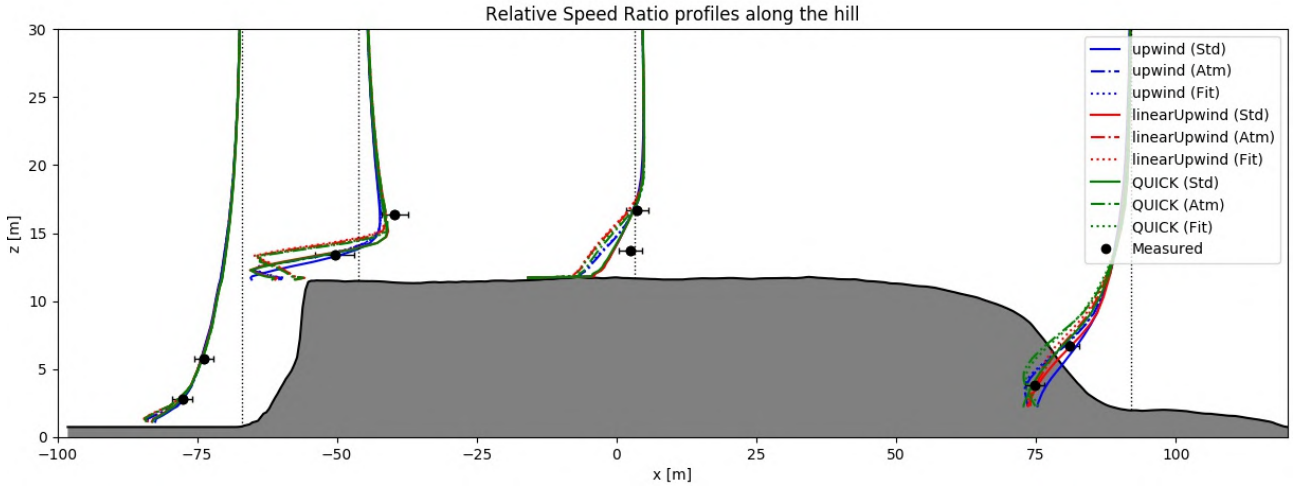

Figure 6. Vertical SR profiles along the Bolund computational domain.

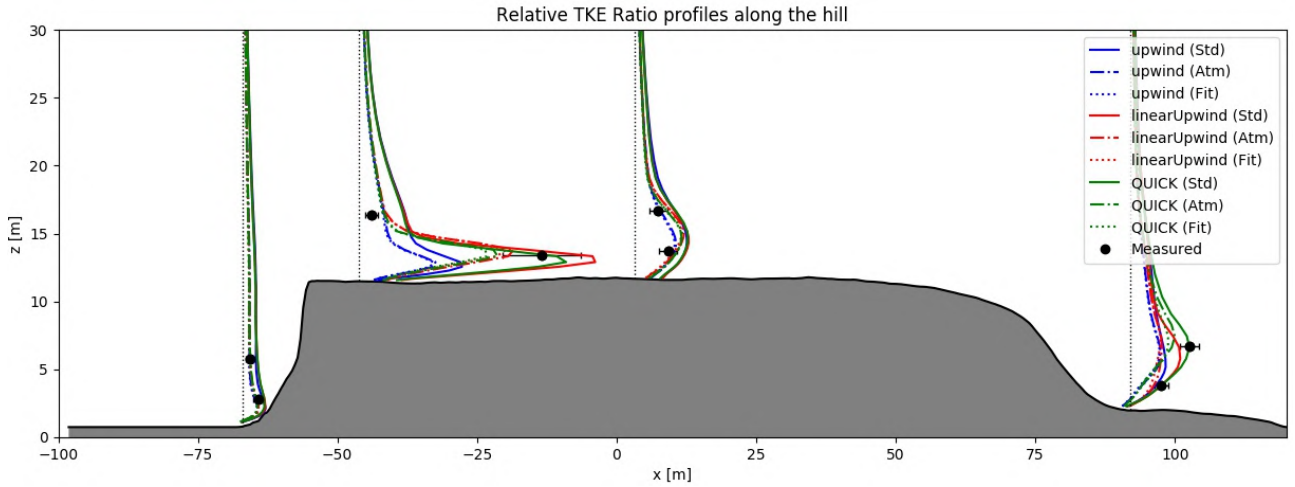

Figure 7. Vertical TKER profiles along the Bolund computational domain.

that the "Atmospheric" set of constants presented the best hit rates for the SR, while underpredicting the TKER at the lee side. Overall, the relation between the SR and TKER fields shown in the simulations was somewhat inconsistent with the measured values, as the simulations with the highest hit rates for SR consistently showed lower hit rates for the TKER.

It was determined that for both hills the model showed minimal grid sensitivity in the regions with attached flow, namely until the lee region for Askervein and until the flow hits the scarp face for Bolund. Outside of those regions, greater mesh refinement led to smaller errors for both SR and TKER at the lee side of the hills. However, as grid refinement greatly increased the gradients close to the ground at the Bolund scarp face, the simulations with more refined grids displayed significant SR underpredictions and thus a better performance by the more diffusive upwind scheme in this region.

In general, particularly for regions above 2 m from the ground, simulations that employed the "Atmospheric" set of

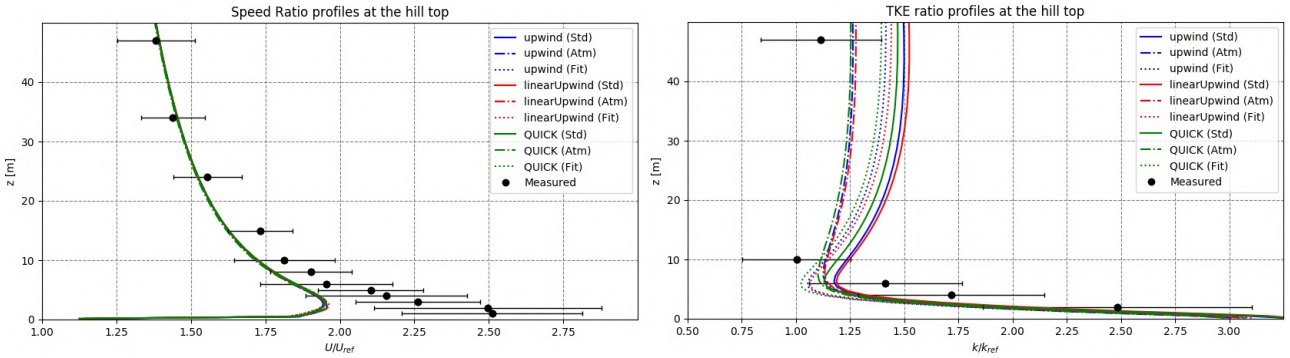

Figure 8. Vertical SR and TKER profiles at the Askervein computational domain hilltop.

constants for the $k-\varepsilon$ model and higher-order divergence schemes presented wind profiles that were in better agreement with the measured data, especially in terms of the SR, which tends to be the most relevant parameter in microscale wind flow studies.

6. ACKNOWLEDGEMENTS

The authors would like to thank Taylor and Teunissen (1987) and (Berg et al., 2011) for conducting the Askervein Hill and Bolund Hill measurement campaigns and providing the data from these projects, as well as the Brazilian National Council for Scientific and Technological Development (CNPq).

7. REFERENCES

Balogh, M., Parente, A. and Benocci, C., 2012. "Rans simulation of abl flow over complex terrains applying an enhanced $k-\varepsilon$ model and wall function formulation: Implementation and comparison for fluent and openfoam". *Journal of Wind Enginnering and Industrial Aerodynamics*, Vol. 104-106, pp. 360–368.

Bechmann, A., Sorensen, N.N., Berg, J., Mann, J. and Réthoré, P.E., 2011. "The bolund experiment, part ii: Blind comparison of microscale flow models". *Boundary-Layer Meteorology*, Vol. 141, pp. 245–271.

Beljaars, A.C.M., Walmsley, J.L. and Taylor, P.A., 1987. "A mixed spectral finite-difference model for neutrally stratified boundary-layer flow over roughness changes and topography". *Boundary-Layer Meteorology*, Vol. 38, pp. 273–303.

Berg, J., Mann, J., Bechmann, A., Courtney, M. and Jorgensen, H.E., 2011. "The bolund experiment, part i: Flow over a steep, three-dimensional hill". *Boundary-Layer Meteorology*, Vol. 141, pp. 219–243.

Jackson, P.S. and Hunt, J.C.R., 1975. "Turbulent windflow over a low hill". *Quarterly Journal of the Royal Meteorology Society*, Vol. 101, pp. 929–955.

Launder, B.E. and Spalding, D.B., 1974. "The numerical computation of turbulent flows". *Computer Methods in Applied Mechanics and Engineering*, Vol. 3, pp. 269–289.

Raithby, G.D., Stubley, G.D. and Taylor, P.A., 1987. "The askervein hill project: A finite control volume prediction of three-dimensional flows over the hill". *Boundary-Layer Meteorology*, Vol. 39, pp. 247–267.

Richards, P.J. and Hoxey, R., 1993. "Appropriate boundary conditions for computational wind engineering models using the $k-\varepsilon$ turbulence model". *Journal of Wind Enginnering and Industrial Aerodynamics*, Vol. 47, pp. 145–153.

Richards, P.J. and Norris, S.E., 2011. "Appropriate boundary conditions for computational wind engineering models revisited". *Journal of Wind Enginnering and Industrial Aerodynamics*, Vol. 99, pp. 257–266.

Schmidt, J., Peralta, C. and Stoevesandt, B., 2012. "Automated generation of structured meshes for wind energy applications". In *Proceedings of the Open Source CFD International Conference*. London, UK.

Stull, R., 1988. *An Introduction to Boundary Layer Meteorology*. Kluwer Academic Publishers, Netherlands, 1st edition.

Taylor, P. and Teunissen, H., 1987. "The askervein hill project: overview and background data". *Boundary-Layer Meteorology*, Vol. 39, pp. 15–39.

8. RESPONSIBILITY NOTICE

The authors are solely responsible for the printed material included in this paper.